Korean J. Chem. Eng., 32(2), 239-247 (2015)
DOI: 10.1007/s11814-014-0225-x

pISSN: 0256-1115
eISSN: 1975-7220

Numerical simulation of CO_2 diffusion and reaction into aqueous solutions of different absorbents

Antonio Comite*, Camilla Costa*, Renzo Di Felice,†, Paolo Pagliai**, and Dario Vitiello****

*Dipartimento di Chimica e Chimica Industriale, Università degli Studi di Genova,
Via Dodecaneso, 31, Genova 16146, Italy
**Dipartimento di Ingegneria Civile Chimica ed Ambientale, Università degli Studi di Genova,
Via Opera Pia, 15, Genova 16145, Italy
(*Received 13 June 2014 • accepted 4 August 2014*)

Abstract–A numerical model comprising a system of partial differential equations was set up to describe the diffusion and reaction of carbon dioxide into aqueous solutions of different absorbents. The solution of the governing equation was a function of the physical and chemical parameters involved, such as Henry constant, diffusion coefficients and reaction rates. Although these parameters have been estimated and reported in literature, uncertainty still exists about their reliability. Comparison between numerical predictions and experimental values from specifically designed experiments shows them to be in good agreement, thus increasing the confidence on the correctness of these parameters, which form then the basis for a proper design of industrial units.

Keywords: CO_2 Capture, Reaction, Diffusion, Henry Constant, Modeling, Membrane

INTRODUCTION

Carbon dioxide discharge into the atmosphere is still on the rise. Even if there is a heated debate on what are the short and long term effects of such discharge, carbon dioxide concentration in the atmosphere is definitely increasing and countermeasures are being devised in order to mitigate this problem. Removal of flue carbon dioxide produced by power plants is one of the actions being considered and, in spite of the relevant technical and economical obstacles, it represents the nearest to industrial applications nowadays available.

Methods to remove carbon dioxide from a gas stream include absorption by a liquid solvent or a suitable solid sorbent, or separation, for example by membranes, of the gas mixture components so that a pure CO_2 stream is captured and then stored. Among these methods, the most used in industry is the reactive adsorption by a liquid absorbent and attention will be concentrated here on such process.

In this type of process carbon dioxide is preferentially dissolved into a liquid phase, where the extent of reaction with a specific sorbent is such that, even if the saturation concentration is relatively small, a large amount of CO_2 can be incorporated into the liquid solution before the regeneration step is carried out. Ethanolammine (MEA) is the most commonly used absorbent; however, because of the health risk associated to operation with such solvent, other non-organic species are also being considered: these include carbonate salts or innovative compounds such as piperazine.

The effectiveness of the CO_2 capture step will depend primarily on the physical and chemical parameters characterizing the adsorbing systems, namely CO_2 solubility, CO_2 diffusion in the gas and liquid phases, and CO_2 reaction rate with the specific absorbent component. These parameters need to be known with the highest possible accuracy to achieve the correct design of the carbon dioxide capture unit. The recent scientific literature is rich with CO_2 capture process simulations where physical and chemical parameters constitute the basis of the numerical calculations, see, e.g. [1,2].

The empirical evaluation of the characteristic physical and chemical parameters that are involved in the absorption of CO_2 by a liquid solution is not trivial; in fact, during the process, carbon dioxide will diffuse through the liquid and also react with one or more components within the liquid phase. As a consequence, if for example CO_2 solubility needs to be determined experimentally, then a precise quantification of all the chemical equilibria in the absorbing solution must be known in order to infer the exact amount of free CO_2 present in the liquid; indeed, such quantity can be quite different from the overall CO_2 absorbed [3].

Moreover, the experimental estimation of the CO_2 diffusivity is even more complex. In fact, researchers, by employing the NO_2 similarity, that is, that NO_2 diffusivity was actually measured rather than CO_2 diffusivity, took advantage of the very similar chemical structure of the two compounds and, therefore, simply assumed that the ratio of diffusivity between the two compounds is constant both in pure water and in a reacting aqueous solution [4-7]. In regards of the experimental determination of the kinetic law, next to the problem already discussed, a further complication arises from the fact that the reaction rate will depend, in principle, on both CO_2 and absorbent concentrations in the liquid phase. This difficulty was overcome, as reported in the majority of cases, by assuming a first-order overall apparent reaction [8-10]; thus, the value of the kinetic constant is relatively simply calculated from the measured

†To whom correspondence should be addressed.
E-mail: renzo.difelice@unige.it

quantities. Nonetheless, when such an assumption cannot be considered valid, then an approximate numerical solution should be searched, as reported, for example, by Derks et al. [10], who made use of the DeCoursey [11] simplified numerical expression.

In this paper, an experimental setup is specifically arranged to measure the transient rate of absorption of carbon dioxide by various aqueous solutions. To this aim, a membrane contactor is employed to obtain a well-defined gas-liquid interface. The liquid phase is maintained static so that any possible fluid dynamic effects on the rate of reaction can be safely discarded. The experimental results are numerically simulated with the exact governing relationships to test the validity of the physical and chemical parameters involved; particularly, the solubility, diffusivity and reaction rate of CO_2 in aqueous solutions of specific sorbents are tested.

We take here a similar approach to other previous works, such as those by Al-Marzouqi et al. [12] and Shirazian et al. [13], who modelled CO_2 absorption in membrane contactors. Compared to those works, however, unsteady-state situations are dealt with here rather than steady-state, thus introducing the time dependency in the mass balance equations.

EXPERIMENTAL SETUP

The experimental setup adopted in this study consists of a particular type of absorbing device, the membrane contactor, on which abundant scientific information is available in the literature [14-17].

In general, such a system is characterized by a microporous hydrophobic membrane that provides the contact between gas and liquid absorbent without dispersing one phase into another. Mass transfer occurs as the solute gas diffuses through the membrane and is absorbed by the liquid solvent.

In this specific arrangement (Fig. 1) a known amount of absorbing liquid solution, 4 liters, was charged into the vessel; then, starting at time zero, a measured gas flux was passed through the membrane while both temperature and pressure were kept at ambient conditions (25 °C). The amount of CO_2 absorbed at selected times was inferred from the measurement of the total gas volumetric flow rate (carried out with a flow meter), and the difference in CO_2 concentration between the inlet and outlet streams, which are determined by means of chromatography. Importantly, to be able to exactly mimic the present process numerically, the liquid was not agitated.

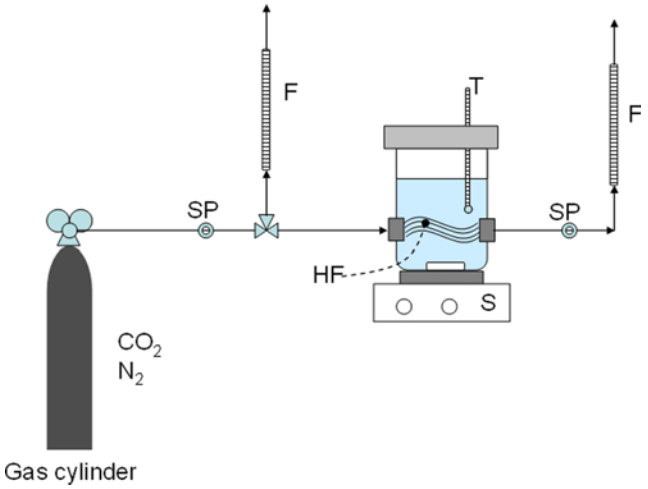

Fig. 1. Experimental setup for absorption of CO_2 in aqueous solutions.
SP. Sampling port
T. Thermometer
S. Magnetic stirrer
F. Flow meter
HF. Hollow fiber

Table 1. Main characteristics of the membrane employed in the experimental set up

Material	Polypropylene
Average pore size	0.2 μm
Porosity (ε)	60%
Inner diameter (d_i)	1.8 mm
Outer diameter (d_o)	1.6 mm
Thickness	0.4 mm
Fiber length	250 mm
Number of fiber	4
Overall interfacial membrane-liquid area	8160 mm^2

A polypropylene hollow fiber was selected as module construction because of its commercial availability, cheapness and relatively high hydrophobicity. Table 1 summarizes the main characteristics of this membrane, which was characterized in a previous work [18].

A gas mixture, containing CO_2 and N_2 in proportion similar to a typical flue gas from a coal combustion plant, flowed into the membrane lumen. The liquid absorbing mixtures being tested were aqueous solutions of monoethanolamine (MEA), potassium carbonate (K_2CO_3) and Piperazine (PZ), respectively. Such reactive components were selected according to their actual or potential industrial use.

The operating conditions set are listed in Table 2.

MATHEMATICAL MODEL

A two-dimensional representation is quite accurate to describe the system under consideration and a schematic diagram is depicted in Fig. 2.

The system is symmetrical relative to the membrane lumen centreline, represented in Fig. 2 by the dot-dash line. The z coordinate indicates direction along the lumen axis, whereas the x coordinate is perpendicular to the membrane itself. Three areas are depicted: the membrane lumen, where the gas mixture flows in the z direction, the membrane wall where the gas component diffuse

Table 2. Operating conditions for the CO_2 absorption tests

Temperature	25 °C
Pressure	Ambient
Inlet CO_2 content	15% v/v
Gas flow rate	3.3×10^{-6} m^3/s
MEA concentration	0.025 $kmol/m^3$
PZ concentration	0.025 $kmol/m^3$
K_2CO_3 concentration	2.75 $kmol/m^3$

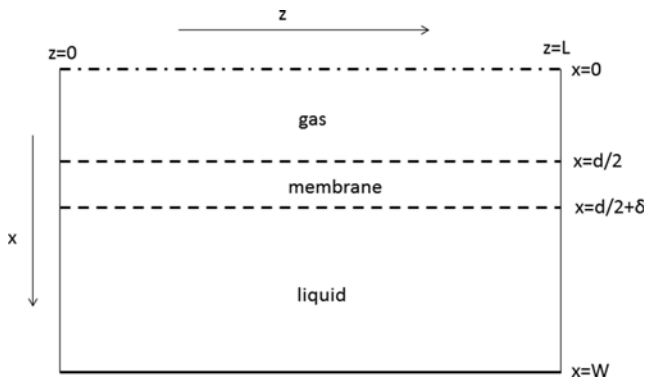

Fig. 2. Schematic representation of the system.

and the confined liquid phase, where the CO_2 diffuses and reacts. It is assumed that the membrane operates under non-wetting condition, i.e., the liquid phase is not penetrating through the membrane wall. This assumption is quite reasonable in light of the hydrophobicity of the membrane material.

In the first region, 0<x<d/2, where the gas flows inside the membrane lumen, CO_2 is the only relevant component and the unsteady-state mole balance is given by:

$$\frac{\partial C_{CO_2,G}}{\partial t}+u_G\frac{\partial C_{CO_2,G}}{\partial z}=D_{CO_2,G}\left[\frac{\partial^2 C_{CO_2,G}}{\partial z^2}+\frac{\partial^2 C_{CO_2,G}}{\partial x^2}\right] \tag{1}$$

In the membrane wall, d/2<x<d/2+δ, CO_2 is again the only relevant component and, neglecting any transport in the z direction, the mole balance is

$$\frac{\partial C_{CO_2,M}}{\partial t}=D_{CO_2,M}\frac{\partial^2 C_{CO_2,M}}{\partial x^2} \tag{2}$$

In the liquid phase, d/2+δ<x<W, both CO_2 and the reacting components, here indicated generically with B, are to be quantified so at least two mass balances are needed:

$$\frac{\partial C_{CO_2,L}}{\partial t}=D_{CO_2,L}\left[\frac{\partial^2 C_{CO_2,L}}{\partial z^2}+\frac{\partial^2 C_{CO_2,L}}{\partial x^2}\right]+r_{CO_2} \tag{3}$$

and

$$\frac{\partial C_{B,L}}{\partial t}=D_{B,L}\left[\frac{\partial^2 C_{B,L}}{\partial z^2}+\frac{\partial^2 C_{B,G}}{\partial x^2}\right]+r_B \tag{4}$$

Continuity and equilibrium at the two interfaces imply that for the gas-membrane interface at x=d/2

$$C_{CO_2,G}=C_{CO_2,M} \tag{5}$$

$$D_{CO_2,G}\frac{\partial C_{CO_2,G}}{\partial x}=D_{CO_2,M}\frac{\partial C_{CO_2,M}}{\partial x} \tag{6}$$

whereas at the membrane-liquid interface, x=d/2+δ,

$$C_{CO_2,M}=mC_{CO_2,L} \tag{7}$$

$$D_{CO_2,M}\frac{\partial C_{CO_2,M}}{\partial x}=D_{CO_2,L}\frac{\partial C_{CO_2,L}}{\partial x} \tag{8}$$

with m being the carbon dioxide partition coefficient between gas and liquid phases, which can be derived from the widely available Henry coefficient H,

$$m=\frac{H}{RT} \tag{9}$$

Initial and boundary conditions need also to be defined. Initial conditions, at t=0, are rather straightforward: no CO_2 is present in the gas, in the membrane and in the liquid phases, so for any z we can write

$$C_{CO_2,G}=0 \qquad \text{for } 0<x<d/2 \tag{10}$$

$$C_{CO_2,M}=0 \qquad \text{for } d/2<x<d/2+\delta \tag{11}$$

$$C_{CO_2,L}=0 \qquad \text{for } d/2+\delta<x<W \tag{12}$$

while in the liquid phase, the component B is present at its initial concentration:

$$C_{B,L}=C^0_{B,L} \qquad \text{for } d/2+\delta<x<W \tag{13}$$

Boundary conditions are defined by considering the symmetry relative to the lumen centerline and the non-permeability of the walls. Thus, we obtain:

at x=0 and for any z

$$D_{CO_2,G}\frac{\partial C_{CO_2,G}}{\partial x}=0 \tag{14}$$

at x=W for any z

$$D_{CO_2,L}\frac{\partial C_{CO_2,L}}{\partial x}=0 \tag{15}$$

$$D_{B,L}\frac{\partial C_{B,L}}{\partial x}=0 \tag{16}$$

As the membrane can also be assumed to be non-permeable to the component B, we accordingly define that for any z and at x=d/2+δ

$$D_{B,L}\frac{\partial C_{B,L}}{\partial x}=0 \tag{17}$$

Finally, for z=0 and z=L we can write

$$D_{CO_2,G}\frac{\partial C_{CO_2,G}}{\partial z}=0 \qquad \text{for } 0<x<d/2 \tag{18}$$

$$D_{CO_2,M}\frac{\partial C_{CO_2,M}}{\partial z}=0 \qquad \text{for } d/2<x<d/2+\delta \tag{19}$$

$$D_{CO_2,L}\frac{\partial C_{CO_2,L}}{\partial z}=0 \qquad \text{for } d/2+\delta<x<W \tag{20}$$

$$D_{B,L}\frac{\partial C_{B,L}}{\partial z}=0 \qquad \text{for } d/2+\delta<x<W \tag{21}$$

NUMERICAL RESULTS AND DISCUSSION

The set of partial differential equations can be integrated with appropriate initial and boundary conditions in order to obtain, as a function of time and position, the values of the component concentration of interest. From these values, the magnitude of the CO_2 flux towards the absorbing solution can be easily estimated and

compared with the experimental results. A specific in-house solver was written in Matlab language in order to solve the system of partial differential equations.

Numerical modelling requires the quantification of the constants populating the system of equations. From the size of the experimental rig, the following geometrical constants were defined (see Fig. 2): L=250 mm, d=1.8 mm, δ=0.4 mm, W=100 mm. Moreover, as in the areas defined by the membrane lumen and the membrane wall itself we are interested only in the determination of the CO_2 concentration profiles, the relevant governing equations are identical regardless of the absorbing solution utilized. Accordingly, the only numerical parameters that need quantification are the CO_2/N_2 diffusion coefficient, which can be easily retrieved from literature and found to be equal to 1.6 10^{-5} m^2/s at ambient conditions, and the CO_2 effective diffusion coefficient in the membrane. The latter requires some simplifying assumptions, as indicated in a previous work on the same membrane from our research group [18], and it was estimated at 1.6 10^{-6} m^2/s.

1. The MEA Absorbing System

In Fig. 3, results expressed in form of CO_2 removal efficiency are summarized for an experimental run using a solution of MEA as absorbing media. In complete agreement with the expected behavior, it can be clearly observed the decay of the efficiency with time.

To model such a specific phenomenon numerically, further physical and chemical parameters need to be defined. The first parameter is the CO_2 partition coefficient at the gas-liquid interface, which can be inferred from the Henry constant, the latter being a known function of MEA concentration and temperature [3]

$$H = 10^{(10.3+0.035C_{MEA}-1140/T)} \tag{22}$$

Calculation for the actual experimental conditions yields a value of 3,032 kPa m^3/kmol.

The second term, namely the carbon dioxide diffusivity in MEA solution, was estimated 1.92 10^{-9} m^2/s, by following the results reported by Ko et al. [4].

Reaction kinetic has been suggested to follow a zwitterion mechanism with the limiting step given by the reaction between CO_2 and MEA itself with a rate law

$$r_{CO_2} = -kC_{CO_2}C_{MEA} \tag{23}$$

and

$$r_{MEA} = 2r_{CO_2} \tag{24}$$

Hikita [8] found

$$\log(k) = 10.99 - \frac{2152}{T} \tag{25}$$

so that we obtain k=5,850 m^3/(kmol s).

The reaction between MEA and CO_2 is an equilibrium reaction, so strictly speaking we should consider the contribution of the reverse reaction also in the kinetic law, Eq. (23). There is however ample evidence [19,20] that for the specific condition reported here, with the system working at ambient temperature, only the forward reaction is relevant. Should we be working at higher temperature, Eq. (23) would have to be modified accordingly, as indicated for example in their seminal work by Astarita and Savage [21].

Finally, MEA diffusivity is inferred from the relation suggested by Snaijder et al. [22]

$$\ln(D_{MEA}) = -13.527 - \frac{2198.3}{T} - 7.8142\ \ 10^{-5}C_{MEA} \tag{26}$$

yielding an estimate value of 1.08 10^{-9} m^2/s.

By inserting these parameters into the system of partial differential equations, CO_2 and MEA concentration profiles were obtained as a function of position, along both x and z coordinates, and time. However, the systems studied showed very little change along the axial direction (CO_2 removal efficiency was only few percent, Fig. 3, and consequently concentrations hardly exhibited any

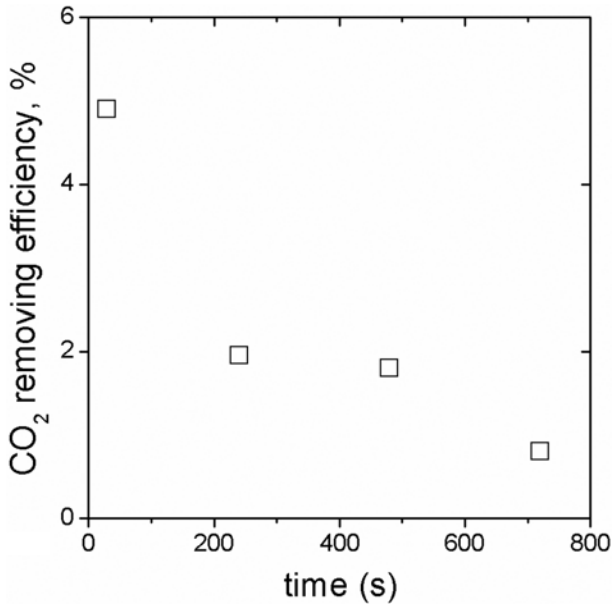

Fig. 3. Measured CO_2 capture efficiency for the MEA absorbing system.

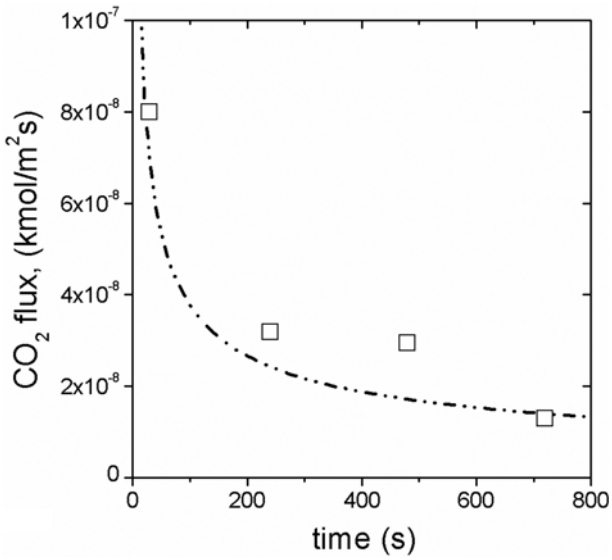

Fig. 4. Experimental and calculated CO_2 flux for the MEA absorbing system.

significant variation along the z direction) and therefore concentration profiles presented later will be depending only on the radial position and on the time.

Data processing allowed, for instance, the average CO_2 flux from the membrane to the liquid solution to be estimated, and the comparison with experimental observations, obtained utilizing measured carbon dioxide removal efficiency, is reported in Fig. 4.

The agreement between calculated and observed fluxes is quite satisfactory, not only qualitatively but also quantitatively. The sharp decline of CO_2 flux with time is physically justified by considering that, as the MEA nearer the membrane get consumed by the reaction, CO_2 has to diffuse a longer distance before reacting, and therefore the overall process is slower. The relevance of this decay can be better appreciated if we concentrate on the first few seconds of the phenomenon, as depicted in Fig. 5.

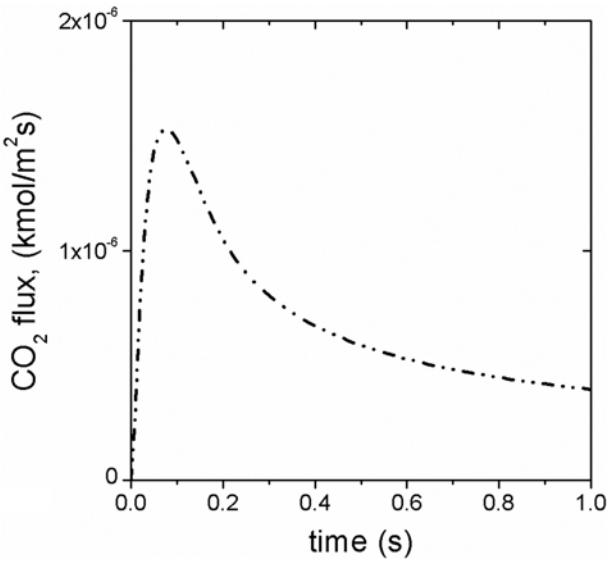

Fig. 5. Initial CO_2 flux for the MEA absorbing system.

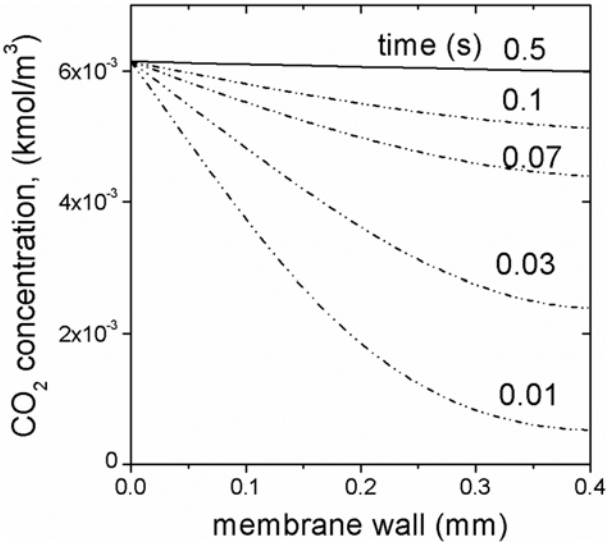

Fig. 6. Calculated CO_2 concentration profiles in the membrane for the MEA absorbing system.

The maximum flux is observed practically straight away, at t= 0.1 s, and it is about two orders of magnitude larger than the one observed after 100 s.

Fig. 6 reports the unsteady-state CO_2 concentration in the membrane wall. Two important observations can be drawn from analyzing the results in Fig. 6: first, the membrane fills up very rapidly (i.e., less than one-tenth of a second) with carbon dioxide; second, the transport resistance inside the membrane is negligible compared to the other mass transfer resistances which develop during the process, this assertion being demonstrated by the flat final CO_2 concentration profile.

Concentration profiles in the liquid phase, at axial z coordinate half of the membrane length, are reported at various times for CO_2 and MEA in Fig. 7 and Fig. 8, respectively. It should be noted how

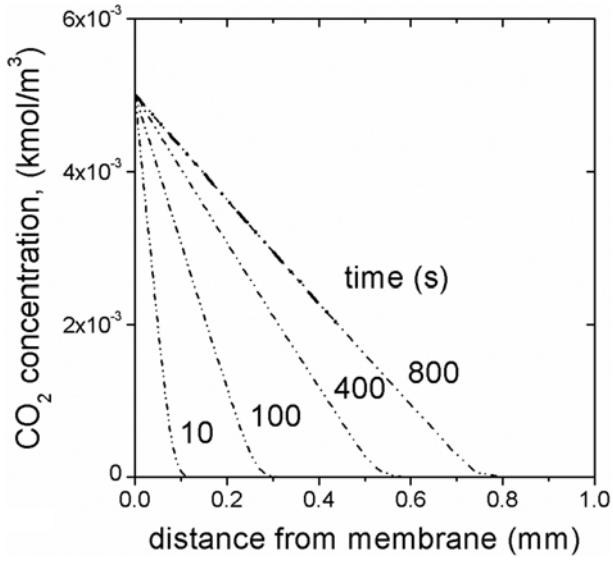

Fig. 7. Calculated CO_2 concentration profiles in the liquid phase for the MEA absorbing system.

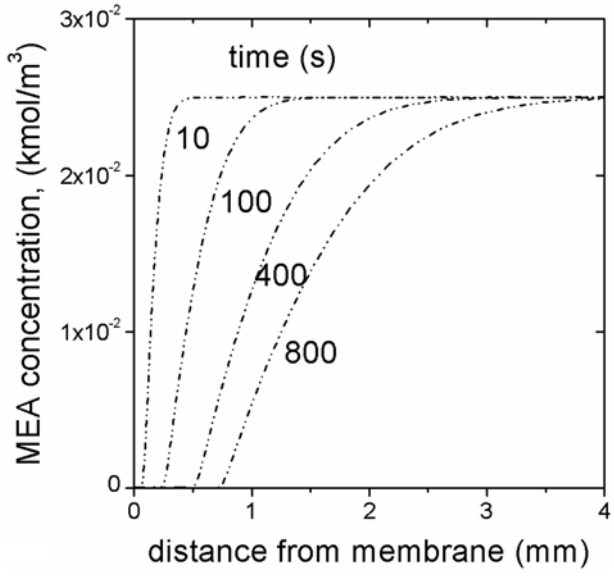

Fig. 8. Calculated MEA concentration profiles in the liquid phase.

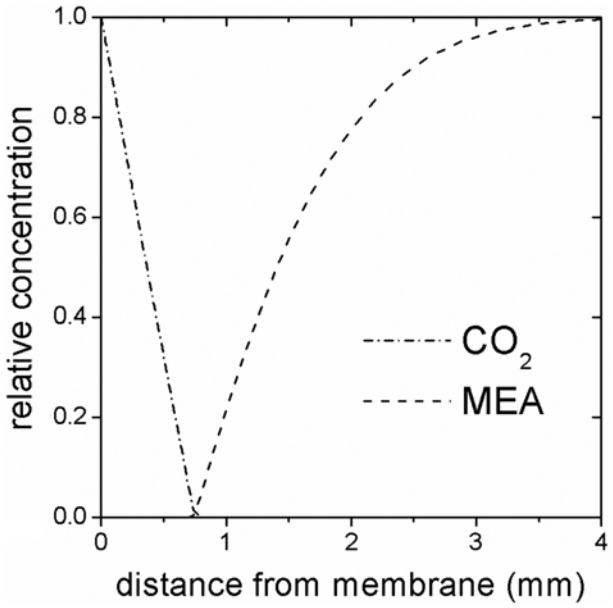

Fig. 9. Calculated CO_2 and MEA concentration profiles in the liquid phase at time=800 s.

slowly the CO_2 is progressing inside the liquid; for the largest time considered, t=800 s, carbon dioxide is not present if we move more than 1 mm away from the membrane interface.

In Fig. 9 the concentration profiles for the two components, made dimensionless by dividing for the boundary values, are reported for one specific time, t=800 s. It is interesting that only a small overlapping region is present, about 0.1 mm in width, which represents the reaction zone, as both concentrations are falling roughly to zero at the same position. Therefore, it can be concluded that the reaction is, in this case, much faster than the diffusion, which is the true limiting rate step that controls the overall reaction.

2. The Piperazine Absorbing System

Piperazine is an etherocycle compound with two N atoms in position 1,4. It is used in alternative to MEA as reactive component for CO_2 absorption because of its potential economic and health safety advantages. The extent of CO_2 removal was experimentally obtained as in the previous case, and results are summarized in Fig. 10.

To carry out the numerical simulation, available data from literature were used. The Henry constant was calculated by linear fitting of published data [6] according to the following relationship:

$$H_{CO_2}=3004.5+226.4C_{PZ} \quad (27)$$

CO_2 diffusivity in PZ solution was obtained from [6]

$$D_{CO_2}=2\ 10^{-9}-3\ 10^{-10}C_{PZ} \quad (28)$$

and PZ diffusivity is estimated by the following [23]:

$$D_{PZ}=1.8D_{MDEA} \quad (28)$$

where

$$\ln(D_{MDEA})=-13.088-\frac{2360.7}{T}-24.727\ \ 10^{-5}C_{MDEA} \quad (29)$$

Indications from previous kinetic studies show that the reaction rate is limited by the second-order reaction between CO_2 and PZ; thus, we can write [10,23]

$$r_{CO_2}=-kC_{CO_2}C_{PZ} \quad (30)$$

with k=72,000 m^3/kmol s at ambient conditions.

According to the experimental PZ concentration, the following values were then estimated: H=3,120 kPa m^3/kmol; $D_{CO_2}=1.99\ 10^{-9}$ m^2/s; $D_{PZ}=1.04\ 10^{-9}$ m^2/s.

The process has been simulated numerically as previously described, and the results, expressed in term of CO_2 flux to the liquid absorbent solution, are reproduced in Fig. 11.

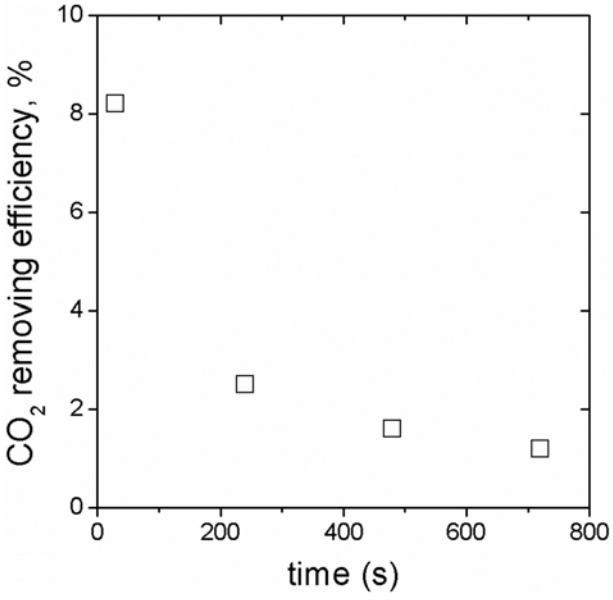

Fig. 10. Measured CO_2 capture efficiency for the PZ absorbing system.

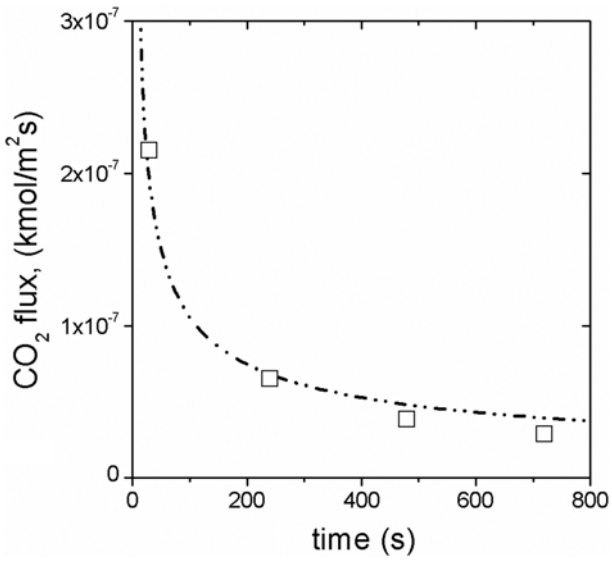

Fig. 11. Experimental and calculated CO_2 flux for the PZ absorbing system.

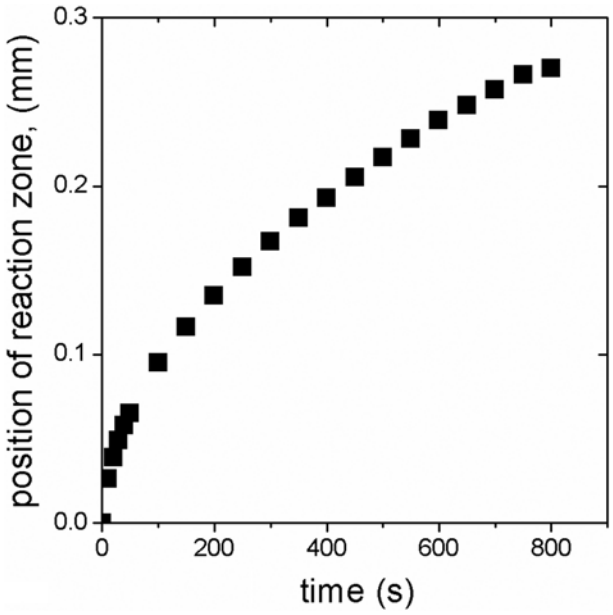

Fig. 12. Position of reaction front for the PZ absorbing system.

Again, a very good agreement between experiment and simulation is obtained. A closer look at the results reported for the Piperazine reveals that CO_2 fluxes are just marginally greater but in the same order of magnitude of those previously reported for the MEA. This would appear surprising given the large difference in reaction rate (more than two orders of magnitude) that exists between the two systems. However, as noted before, and this holds true especially for the Piperazine system, the whole process is limited by the diffusion rather than the reaction: thus, as the relevant diffusion coefficients are very similar, so are the overall process rates.

Concentration profiles at various times were also calculated, but, given their similarity to the previous system, they are not reported for the sake of brevity. The reaction zone is only about 0.03 mm in thickness, thus approaching the case of a reaction plane as expected for an infinitely fast reaction. Numerical simulation allows for the determination of the reaction zone position with time, and this is reported in Fig. 12. Moving from the membrane wall at time equal to zero, the reaction zone is moving away from the membrane-liquid interface at a decreasing velocity. Note that a steady-state value can never be obtained given that the liquid phase is a batch reacting system.

3. The Potassium Carbonate Absorbing System

Concentrated potassium carbonate solutions are sometimes used in industrial applications for CO_2 capture as alternative to ammine solutions. K_2CO_3 is a salt and this makes the process modelling more complicated from a chemistry point of view. When potassium carbonate is dissolved in water it is ionized into K^+ and CO_3^{2-} ions, then bicarbonate ions HCO_3^- and OH^- are formed by hydrolysis:

$$K_2CO_3 \rightarrow 2K^+ + CO_3^{2-} \quad (31)$$

$$CO_3^{2-} + H_2O \rightarrow HCO_3^- + OH^- \quad (32)$$

As reported by many authors [7,24] when CO_2 is absorbed into this solution the following reactions take place:

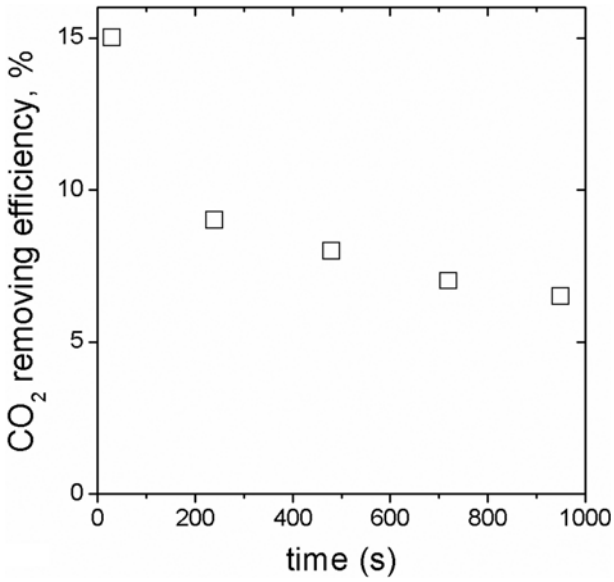

Fig. 13. Measured CO_2 removal efficiency for the K_2CO_3 system.

$$CO_2 + OH^- \rightarrow HCO_3^- \quad (33)$$

$$CO_2 + 2H_2O \rightarrow HCO_3^- + H_3O^+ \quad (34)$$

$$CO_3^{2-} + H_2O \rightarrow HCO_3^- + OH^- \quad (35)$$

$$2H_2O \rightarrow OH^- + H_3O^+ \quad (36)$$

And the overall reaction of carbon dioxide absorption in aqueous carbonate solution is written as:

$$CO_2 + CO_3^{2-} + H_2O \rightarrow 2HCO_3^- \quad (37)$$

The reaction between CO_2 and OH^- is the controlling step, whereas the reaction between CO_2 and H_2O is slow and unimportant in basic solutions [25].

Fig. 13 summarizes the experimental CO_2 removal efficiency for the system in hand. Compared to the previous cases, higher efficiency were found, and this is attributable to the very large carbonate concentration used, which is comparable to the value typical of an industrial unit.

As before, to carry out the numerical simulation, all the physical and chemical parameters need to be estimated.

Henry constant was estimated using Knuutila et al. [7] data and set to 22,708 kPa m^3/kmol. CO_2 diffusivity in the liquid solution was found as 8.55 10^{-10} m^2/s [5], whereas carbonate and hydroxyl ions diffusivity were estimated using Reid et al. [26] empirical expression and equal to 1.87 10^{-9} m^2/s and 1.96 10^{-9} m^2/s, respectively.

The rate-controlling step is second-order according to the law:

$$(-r_{CO_2}) = k[CO_2][OH^-] \quad (38)$$

The reaction rate constant k can be evaluated using the equation proposed by Astarita et al. [27]:

$$\log_{10} k = 13.635 - \frac{2895}{T} + 0.08I \quad (39)$$

where I is the solution ionic strength and T is in K. Therefore, the kinetic constant depends on both the temperature and the ionic

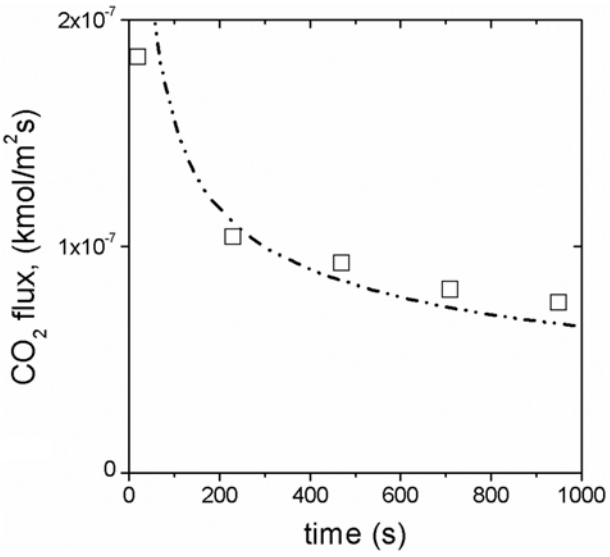

Fig. 14. Measured and calculated CO_2 fluxes for the K_2CO_3 absorbing system.

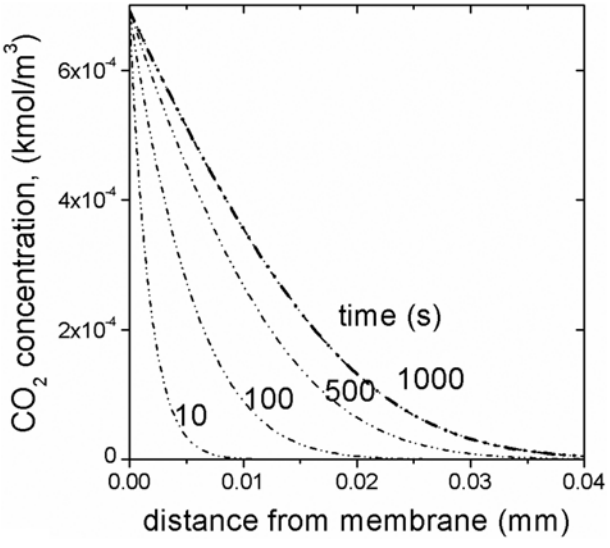

Fig. 15. CO_2 concentration profile in the liquid phase for the K_2CO_3 absorbing system.

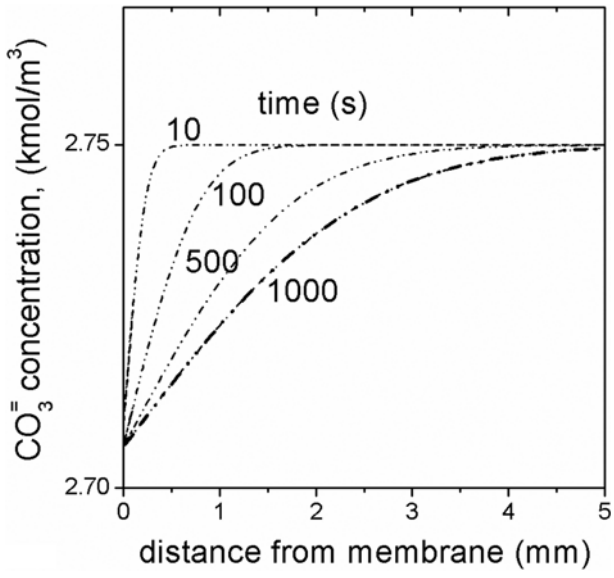

Fig. 16. CO_3^{2-} concentration profile in the liquid phase for the K_2CO_3 absorbing system.

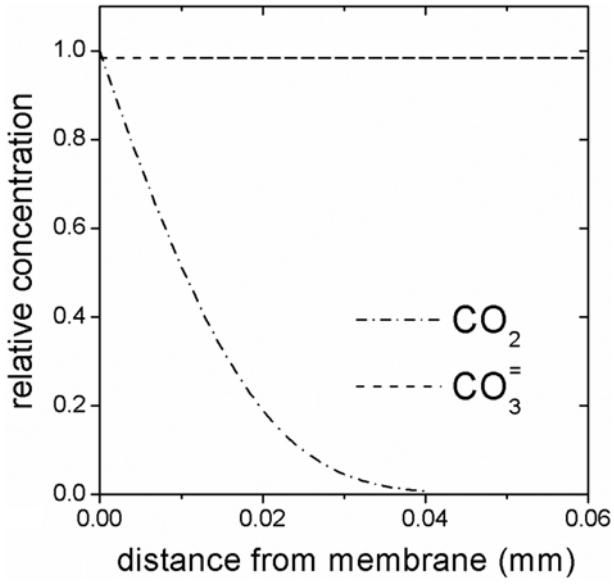

Fig. 17. Reactant concentration profiles in the liquid phase for the K_2CO_3 absorbing system.

strength.

Fig. 14 reports the comparison between the calculated CO_2 flux at different times with the relevant measured values. Similarly to the previous results, the agreement is very good.

Figs. 15 and 16 report the time dependency of the calculated concentration profiles in the liquid phase for the CO_2 and the carbonate ion, respectively. Again the reaction takes place, within the time span investigated, at a very small distance from the membrane wall, and within a region only few hundredth millimeters deep. However, it is also quite evident that these concentration profiles are very different from those presented for the previous systems.

A closer look at Fig. 16 suggests the justification for such different behavior. In fact, the carbonate ion concentration is hardly changing, and it can be practically assumed as constant, i.e., equal to the initial conditions, at any time and any position. This is explained by the presence of a large excess of carbonate reagent in the system, which is a few orders of magnitude larger than the stoichiometric amount. Such a limiting condition is a well-known documented example reported in the reaction engineering text books [28], where the large excess of the absorbent induces the system to behave like on overall first order reaction relative to the diffusing component, i.e., the CO_2 in our case. Fig. 17 depicts the relative concentration profiles of CO_2 and carbonate ions after a time of 1,000 s, which are in perfect agreement with the expected behavior.

For this specific case an analytical solution for the CO_2 flux has been known for a long time, and, by taking into account the mem-

brane porosity, ε, is equal to

$$N_{CO_2} = \frac{\varepsilon p_{CO_2} \sqrt{D_{CO_2} k C_{OH^-}}}{H_{CO_2}} \quad (40)$$

Substituting the proper values into the above equation, a CO_2 flux in the order of 10^{-7} kmol/m^{2}s is obtained, which is in good agreement with measured and numerically calculated values.

CONCLUSIONS

The plugging of published physical and chemical data on carbon dioxide - aqueous absorbent systems into a numerical model has shown a more than satisfactory outcome. The model was able to reproduce unsteady-state CO_2 fluxes in a membrane contactor with three different type of absorbents, the commonly used MEA and, in addition, Piperazine and potassium carbonate. Therefore the validity of these types of data, obtained experimentally by making use of simplifying assumptions, is strengthened, and they can be used more confidently in the design of industrial apparatus.

REFERENCES

1. J. Gáspár and A.-M. Cormoş, *Comput. Chem. Eng.*, **35**, 2044 (2011).
2. S. A. Jayarathna, B. Lie and M. C. Melaaen, *Comput. Chem. Eng.*, **53**, 178 (2013).
3. R. Maceiras, E. Alvarez and M. Cancela, *Chem. Eng. J.*, **138**, 295 (2008).
4. J.-J. Ko, T. C. Tsai, C. Y. Lin, H. M. Wang and M. H. Li, *J. Chem. Eng. Data*, **46**, 160 (2001).
5. A. H. G. Cents, D. W. F. Brilman and G. F. Versteeg, *Chem. Eng. Sci.*, **56**, 1075 (2001).
6. A. Samanta, S. Roy and S. S. Bandyopadhyay, *J. Chem. Eng. Data*, **52**, 1381 (2007).
7. H. Knuutila, O. Juliussen and H. F. Svendsen, *Chem. Eng. Sci.*, **65**, 2177 (2010).
8. H. Hikita, S. Asai and T. Takatsuka, *Chem. Eng. J.*, **13**, 7 (1977).
9. R. Pohorecki and W. Moniuk, *Chem. Eng. Sci.*, **43**, 1677 (1988).
10. P. W. J. Derks, T. Kleingeld, C. van Aken, J. A. Hogendoorn and G. F. Versteeg, *Chem. Eng. Sci.*, **61**, 6837 (2006).
11. W. J. DeCoursey, *Chem. Eng. Sci.*, **29**, 1867 (1974).
12. M. H. Al-Marzouqi, M. H. El-Naas, S. A. M. Marzouk, M. A. Al-Zarooni, N. Abdullatif and R. Faiz, *Sep. Purif. Technol.*, **59**, 286 (2008).
13. S. Shirazian, M. Pishnamazi, M. Rezakazemi, A. Nouri, M. Jafari, S. Noroozi and A. Marjani, *Chem. Eng. Technol.*, **35**, 1077 (2012).
14. J.-L. Li and B.-H. Chen, *Sep. Purif. Technol.*, **41**, 109 (2005).
15. A. Gabelman and S.-T. Hwang, *J. Membr. Sci.*, **159**, 61 (1999).
16. Z. Qi and E. L. Cussler, *J. Membr. Sci.*, **23**, 321 (1985).
17. Z. Qi and E. L. Cussler, *J. Membr. Sci.*, **23**, 333 (1985).
18. A. Bottino, G. Capannelli, A. Comite and R. Di Felice, *Sep. Purif. Technol.*, **59**, 85 (2008).
19. P. M. M. Blauwhoff, G. F. Versteeg and W. P. M. van Swaaij, *Chem. Eng. Sci.*, **39**, 207 (1984).
20. P. D. Vaidya and E. Y. Kenig, *Chem. Eng. Sci.*, **30**, 1467 (2007).
21. G. Astarita and D. W. Savage, *Chem. Eng. Sci.*, **35**, 649 (1980).
22. E. D. Snijder, M. J. Riele, G. F. Versteeg and W. P. M. Van Swaaij, *J. Chem. Eng. Data*, **38**, 475 (1993).
23. A. Samanta and S. S. Bandyopadhyay, *Chem. Eng. Sci.*, **62**, 7312 (2007).
24. V. Y. Dindore, D. W. F. Brilman and G. F. Versteeg, *J. Membr. Sci.*, **255**, 275 (2005).
25. D. W. Savage, G. Astarita and S. Joshi, *Chem. Eng. Sci.*, **35**, 1513 (1980).
26. R. C. Reid, J. M. Prausnitz and B. E. Poling, *The properties of gases and liquids*, McGraw-Hill, Singapore (1988).
27. G. Astarita, D. W. Savage and A. Bisio, *Gas Treating with Chemical Solvents*, Wiley, New York (1983).
28. O. Levenspiel, *Chemical Reaction Engineering*, 2nd Ed. New York, Wiley (1972).